Journal of the Association of Arab Universities for Basic and Applied Sciences (2016) **21**, 24–30

University of Bahrain

Journal of the Association of Arab Universities for Basic and Applied Sciences

www.elsevier.com/locate/jaaubas
www.sciencedirect.com

ORIGINAL ARTICLE

A thermodynamical, electrochemical and surface investigation of Bis (indolyl) methanes as Green corrosion inhibitors for mild steel in 1 M hydrochloric acid solution

Chandrabhan Verma, Pooja Singh, M.A. Quraishi *

Department of Chemistry, Indian Institute of Technology, Banaras Hindu University, Varanasi 221005, India

Received 23 February 2015; revised 20 April 2015; accepted 25 April 2015
Available online 23 May 2015

KEYWORDS

Mild steel;
Corrosion;
EIS;
Tafel polarization;
SEM/EDX

Abstract The influence of three Bis (indolyl) methanes (BIMs) namely, 3,3′-((4-nitrophenyl) methylene) bis (1H-indole) (BIM-1), 3,3′-(phenyl methylene) bis (1H-indole) (BIM-2) and 4-((1H-indol-2-yl)(1H-indol-3-yl) methyl) phenol (BIM-3) on the mild steel corrosion in 1 M HCl was studied by weight loss, electrochemical, scanning electron microscopy (SEM), and dispersive X-ray spectroscopy (EDX) methods. Results showed that BIM-3 shows maximum inhibition efficiency of 98.06% at 200 mg L^{-1} concentration. Polarization study revealed that the BIMs act as mixed type inhibitors. Adsorption of BIMs on the mild steel surface obeyed the Langmuir adsorption isotherm. The weight loss and electrochemical results were well supported by SEM and EDX studies.

1. Introduction

Organic compounds particularly, N-heterocyclic have been reported as effective corrosion inhibitors for mild steel against corrosion during several industrial processes (Solmaz, 2014; Musa et al., 2012; Mahdavian and Ashhari, 2010; Ozkir et al., 2012). Ultrasound irradiation has immerged as a powerful technique for the synthesis of various heterocyclic compounds of industrial and biological interest (Goharshad et al., 2009) due to their shorter reaction time, simple operating procedure, high yield, high selectivity and clean reaction (Joshi et al., 2010).

Indole and its derivatives have received considerable attention of synthetic chemists due to their several biological applications such as antibacterial, cytotoxic, antioxidative, insecticidal activities and bioactive metabolites of terrestrial and marine origin (Surasani et al., 2013). In our present investigation we have synthesized and studied the corrosion inhibition efficiency of three Bis (indolyl) methanes on mild steel corrosion in 1 M HCl. The criteria behind selecting these compounds as corrosion inhibitors were that: (a) they can be easily synthesized from commercially available and relatively cheap starting materials (b) contain –OH, $–NO_2$ and heteroaromatic rings through which they can adsorb and inhibit corrosion (c) they were effective even at low concentration and (d) they were highly soluble in testing medium. Previously, few

* Corresponding author. Tel.: +91 9307025126; fax: +91 542 2368428.
E-mail addresses: maquraishi.apc@itbhu.ac.in, maquraishi@rediffmail.com (M.A. Quraishi).
Peer review under responsibility of University of Bahrain.

http://dx.doi.org/10.1016/j.jaubas.2015.04.003
1815-3852

authors reported the corrosion inhibition efficiency of the indole and its derivatives in acid solution for different metals (Norr, 2008; Popova and Christov, 2006; Lowmunkhong et al., 2010; Quartarone et al., 2008).

2. Experimental section

2.1. Material

The mild steel specimens having composition (wt.%): C = 0.076, Mn = 0.192, P = 0.012, Si = 0.026, Cr = 0.050, Al = 0.023, and remainder Fe were used in present study. The test solution (1 M HCl) was prepared by dilution of analytical grade HCl (MERK, 37%) in double deionized water.

2.2. Synthesis of inhibitors (BIMs)

In the present study Bis (indolyl) methanes (BIMs) were synthesized as described earlier (Sonar et al., 2009). The synthetic rout for BIMs is shown in Scheme 1. The purity of products was determined by TLC method. The characterization data of the synthesized compounds are as follows: BIM-1 (3,3′-((4-nitrophenyl) methylene) bis (1H-indole, –R = –Ph (4-NO_2))): MP: 223-224 °C, IR (KBr, cm^{-1}): 3428, 2829, 2245, 1680–1660, 1522, 1230, 845, 739, 641. BIM-2 (3,3′-(phenyl methylene) bis (1H-indole) –R = Ph): MP: 125–127 °C, IR (KBr, cm^{-1}): 3465, 2811, 2275, 1482, 1130, 825, 758, 611. BIM-3 (4-((1H-indol-2-yl)(1H-indol-3-yl) methyl) phenol, –R = Ph(4-OH)): MP: 123–125 °C, IR (KBr, cm^{-1}): 3623, 3475, 2831, 2356, 1453, 1238, 845, 734, 623.

2.3. Gravimetric experiment

The weight loss experiments in the absence and the presence of different concentrations of BIMs were carried out to optimize the concentration of BIMs as described earlier (Verma et al., 2014). The corrosion rate (C_R), percentage inhibition efficiency ($\eta\%$) and surface coverage (θ) were calculated using following equations.

$$C_R = \frac{87.6W}{A\ t\ d} \quad (1)$$

$$\eta\% = \frac{C_R - C_{R(i)}}{C_R} \times 100 \quad (2)$$

$$\theta = \frac{C_R - C_{R(i)}}{C_R} \quad (3)$$

where, W is the weight loss in mg, A is the area (cm^2) of the mild steel sample exposed to 1 M HCl, t is the immersion time (3 h), d is the density of mild steel (g cm^{-3}) and C_R and $C_{R(i)}$ are the corrosion rates in the presence and the absence of BIMs, respectively.

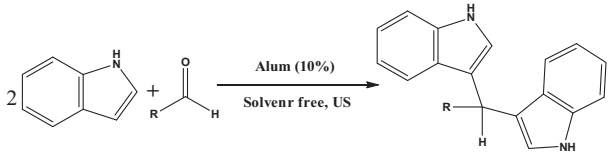

Scheme 1 Synthetic route for investigated BIMs.

2.4. Electrochemical experiments

As described earlier (Verma et al., 2014a), a typical three electrodes glass cell consisting of a highly pure platinum mesh as counter electrode, a saturated calomel as reference electrode and mild steel specimen as working electrode was used for electrochemical studies. The Tafel and EIS measurements were carried out using a Gamry Potentiostat/Galvanostat (Model G-300) with EIS Software Gamry Instruments Inc., USA. Echem Analyst 5.0 Software package was applied to analyze the electrochemical data. The cathodic and anodic Tafel slopes were recorded by changing the electrode potential inevitably from −0.25 to +0.25 V vs. corrosion potential (E_{corr}) at a constant sweep rate of 1.0 mV s^{-1}. The EIS studies were carried out under potentiostatic condition in a frequency range of 100 kHz–0.01 Hz. The amplitude of the AC sinusoid wave was 10 mV. All the Tafel and EIS studies were performed in naturally aerated solution of 1 M HCl in the absence and the presence of 200 mg L^{-1} concentration of BIMs after 30 min immersion time.

2.5. SEM/EDX analysis

The SEM model Ziess Evo 50XVP instrument was used for the mild steel surface analysis with and without BIMs using accelerating voltage of 50 kV at 500× magnifications. Before SEM and EDX analysis the mild steel samples were immersed for 3 h in the absence and the presence of BIMs. The elemental composition was determined using energy dispersive X-ray spectroscopy (EDX) coupled with SEM.

3. Result and discussion

3.1. Weight loss measurements

3.1.1. Effect of concentration

Variation of the inhibition efficiency ($\eta\%$) at different studied concentrations of BIMs is shown in Fig. 1. It is obvious that

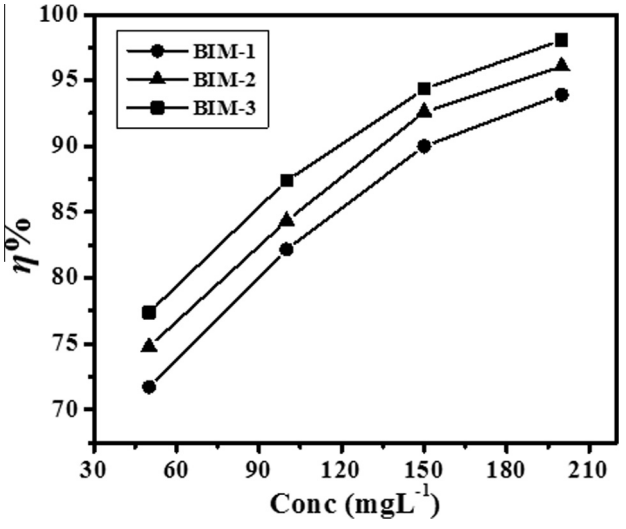

Figure 1 Variation of inhibition efficiency with BIMs concentration of mild steel immersed in 1 M HCl obtained by weight loss measurement.

the values of $\eta\%$ increases on increasing BIMs concentration. The maximum $\eta\%$ was obtained at 200 mg L^{-1} concentration further increase in concentration does not cause any significant change in the inhibition performance suggesting that 200 mg L^{-1} is the optimum concentration. The increase in BIMs concentration increases the surface coverage (θ) through adsorbing on its surface and therefore, increases inhibition efficiency (Yadav et al., 2013).

Table 1 Variation of corrosion rate with temperature in the absence and presence of optimum concentration of BIMs.

Temperature (K)	Corrosion rate (C_R) (mg cm^{-2} h^{-1})			
	Blank	BIM-1	BIM-2	BIM-3
308	7.60	0.46	0.30	0.13
318	11.0	1.23	1.10	0.83
328	14.3	2.03	1.80	1.56
338	18.6	3.30	2.76	2.46

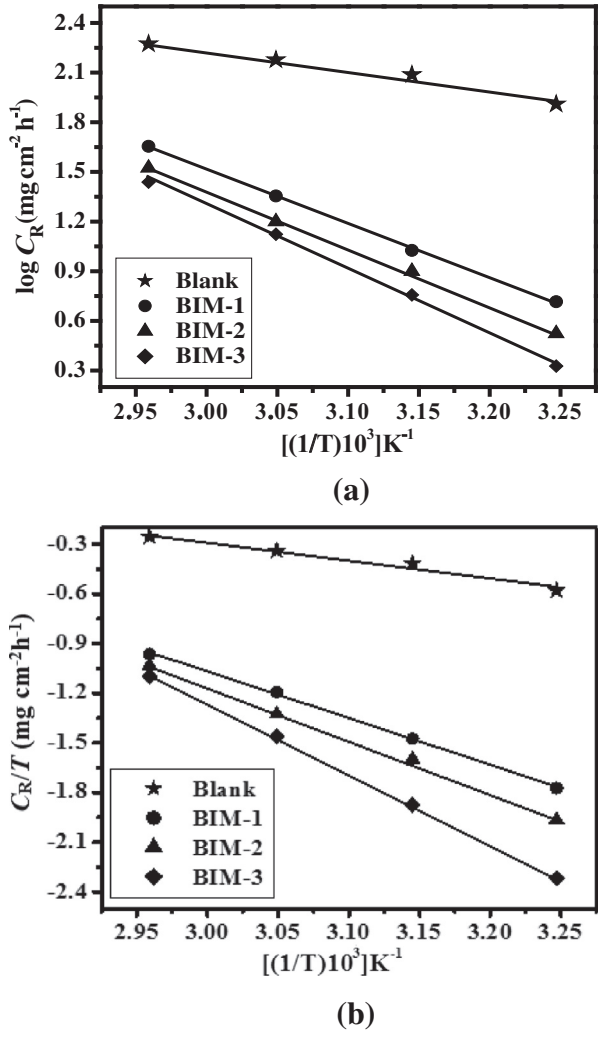

Figure 2 Arrhenius plots for mild steel in 1 M HCl in the absence and presence of different concentrations of BIMs.

3.1.2. Effect of temperature

To investigate the effect of temperature on inhibition performance of BIMs, the weight loss experiments were also performed at different temperatures (308–338 K). The values of the C_R at different studied temperatures are listed in Table 1. It is apparent from results that the value of the C_R increases on increasing temperature for inhibited as well as uninhibited solutions. This increased values of C_R is attributed to desorption of the adsorb BIMs molecules from mild steel surface at elevated temperatures, resulting in enhanced C_R (Barmatov et al., 2015).

The temperature dependency of corrosion rate can be best represented by the Arrhenius and transition state equations (Deng et al., 2011):

$$\log(C_R) = \frac{-E_a}{2.303RT} + \log \lambda \quad (4)$$

$$C_R = \frac{RT}{Nh} \exp\left(\frac{\Delta S^*}{R}\right) \exp\left(-\frac{\Delta H^*}{RT}\right) \quad (5)$$

where, h is Plank's constant, E_a is the apparent activation energy, N is Avogadro's number, ΔS^* is the entropy of activation and ΔH^* is the enthalpy of activation R is the gas constant, T is the temperature, λ is the Arrhenius pre-exponential factor. The values of activation parameter (E_a) and transition state Parameters (ΔH^*, ΔS^*) were calculated from Arrhenius plots (Fig. 2a) and transition state plots

Table 2 Activation parameters for mild steel dissolution in 1 M HCl in the absence and presence of optimum concentration of BIMs.

Inhibitor	E_a (kJ mol^{-1})	ΔH^* (kJ mol^{-1})	ΔS^* (J/mol K)
Blank	28.48	26.04	−148.9
BIM-1	62.72	54.06	147.12
BIM-2	65.83	54.53	−127.5
BIM-3	73.93	72.43	−68.2

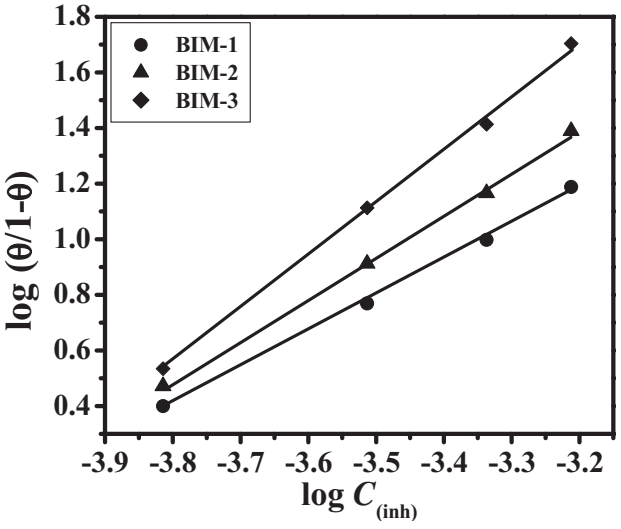

Figure 3 Langmuir isotherm plots for mild steel in 1 M HCl solution containing different concentration of BIMs.

Table 3 The values of K_{ads} and $\Delta G°_{ads}$ for mild steel in the absence and presence of optimum concentration of BIMs in 1 M HCl at different studied temperatures.

Inhibitor	K_{ads} (10^4 M^{-1})				$-\Delta G°_{ads}$ (kJ mol^{-1})			
	308	318	328	338	308	318	328	338
BIM-1	18.43	5.37	3.54	2.37	35.75	34.39	33.53	33.38
BIM-2	20.98	5.87	3.89	2.46	35.98	34.13	33.23	33.35
BIM-3	25.85	6.35	4.65	2.85	36.42	35.52	34.43	33.47

(Fig. 2b), respectively and given in Table 2. The increased value of the E_a in the presence of BIMs is attributed due to physical adsorption that takes place during first step of adsorption processes (Faustin et al., 2015). The positive values of ΔH^* reflect the endothermic nature of mild steel dissolution in acidic medium and the negative values of ΔS^* suggest the formation of activated complex in the rate determining step which represent dissociation rather than association suggesting that disorderness increases on going from reactant to activated complex (Faustin et al., 2015).

3.1.3. Adsorption isotherm and energy of adsorption

In order to gain some mechanistic information about adsorption of BIMs on mild steel surface, several adsorption isotherms such as Langmuir, Temkin, Freundluich, Bockris–Swinkles and Flory–Huggins isotherms were tested.

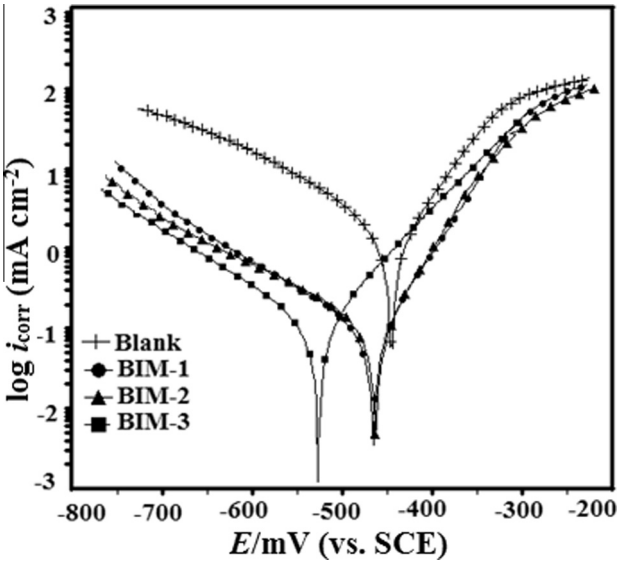

Figure 4 Tafel polarization curves for mild steel obtained in 1 M HCl containing different concentrations BIMs.

Table 4 Tafel Polarization parameters for mild steel in 1 M HCl solution in the absence and presence of optimum concentration of BIMs.

Inhibitor	E_{corr} (V/SCE)	i_{corr} (μA/cm)	β_a (mV/dec)	β_c (mV/dec)	η%
Blank	−445	1150	70.5	114.6	–
BIM-1	−466	95.8	66.8	151.0	91.66
BIM-2	−463	94.1	61.3	138.4	91.82
BIM-3	−527	63.51	80.9	127.9	94.47

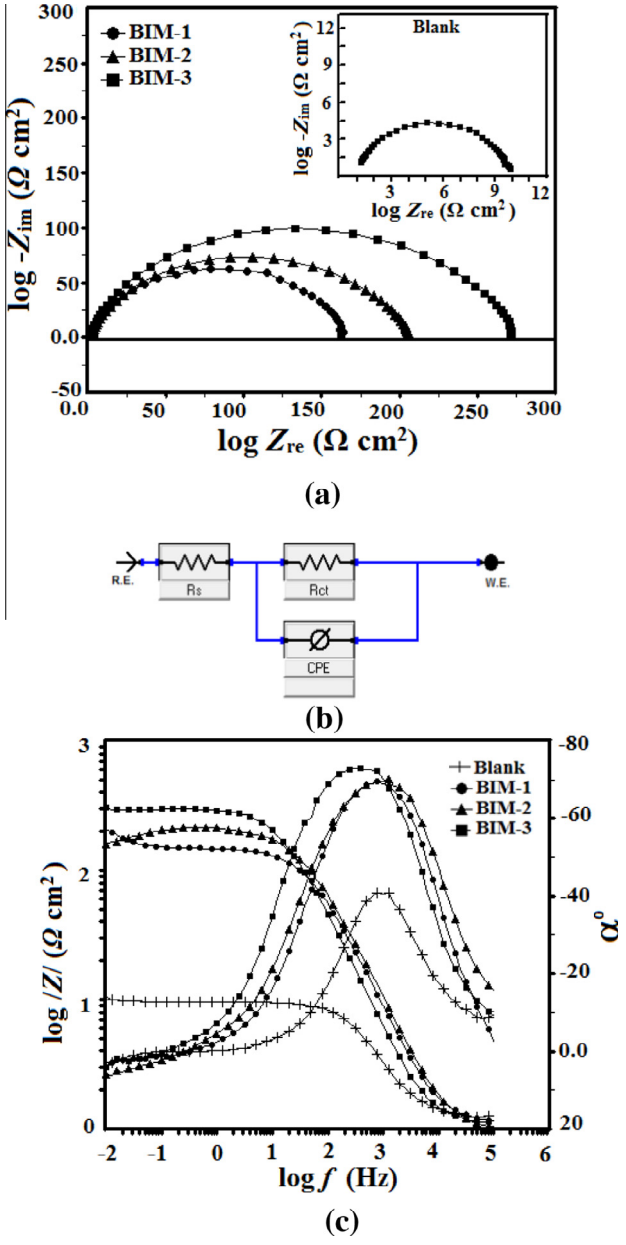

Figure 5 (a) Nyquist plots for mild steel obtained in 1 M HCl containing different concentrations BIMs. (b) Equivalent circuit used to fit the EIS data for mild steel in 1 M HCl.

The surface coverage values (θ) as a function of logarithm of BIMs concentration were tested graphically to obtain the best adsorption isotherm. In our present study the Langmuir isotherm gave the best fit which can be best represented by following equation (Verma et al., 2014b):

$$\frac{C_{(inh)}}{\theta} = \frac{1}{K_{(ads)}} + C_{(inh)} \quad (6)$$

where, $C_{(inh)}$ is the inhibitor concentration and K_{ads} is the equilibrium constant for the adsorption–desorption process. The values of K_{ads} were calculated at different studied temperatures from the intercept of the Langmuir plot shown in Fig. 3 and given in Table 3. The values of K_{ads} related to the free energy of adsorption (ΔG°_{ads}) by following relation (Bahrami et al., 2010):

$$\Delta G^{\circ}_{ads} = -RT \ln (55.5 K_{ads}) \quad (7)$$

The value 55.5 in above equation represents the concentration of water in acid solution in mol L^{-1}. Generally, a higher value of K_{ads} associated with higher tendency to adsorb on mild steel surface. In our present study the K_{ads} value of different BIMs follows the order: BIM-3 > BIM-2 > BIM-1 which is in accordance with the order of the $\eta\%$. In our present

Table 5 Electrochemical impedance parameters obtained from EIS measurements for mild steel in 1 M HCl in the absence and presence of optimum concentration of BIMs.

Inhibitor	R_s (Ω cm^2)	R_{ct} (Ω cm^2)	C_{dl} (μF cm^{-2})	n	$\eta\%$	Goodness of fit
Blank	1.12	9.58	106.21	0.827	–	3.735×10^{-3}
BIM-1	0.73	161.8	36.68	0.827	94.07	1.332×10^{-3}
BIM-2	1.11	199.9	29.99	0.848	95.20	674.1×10^{-6}
BIM-3	1.05	264.4	24.80	0.854	97.44	858.9×10^{-6}

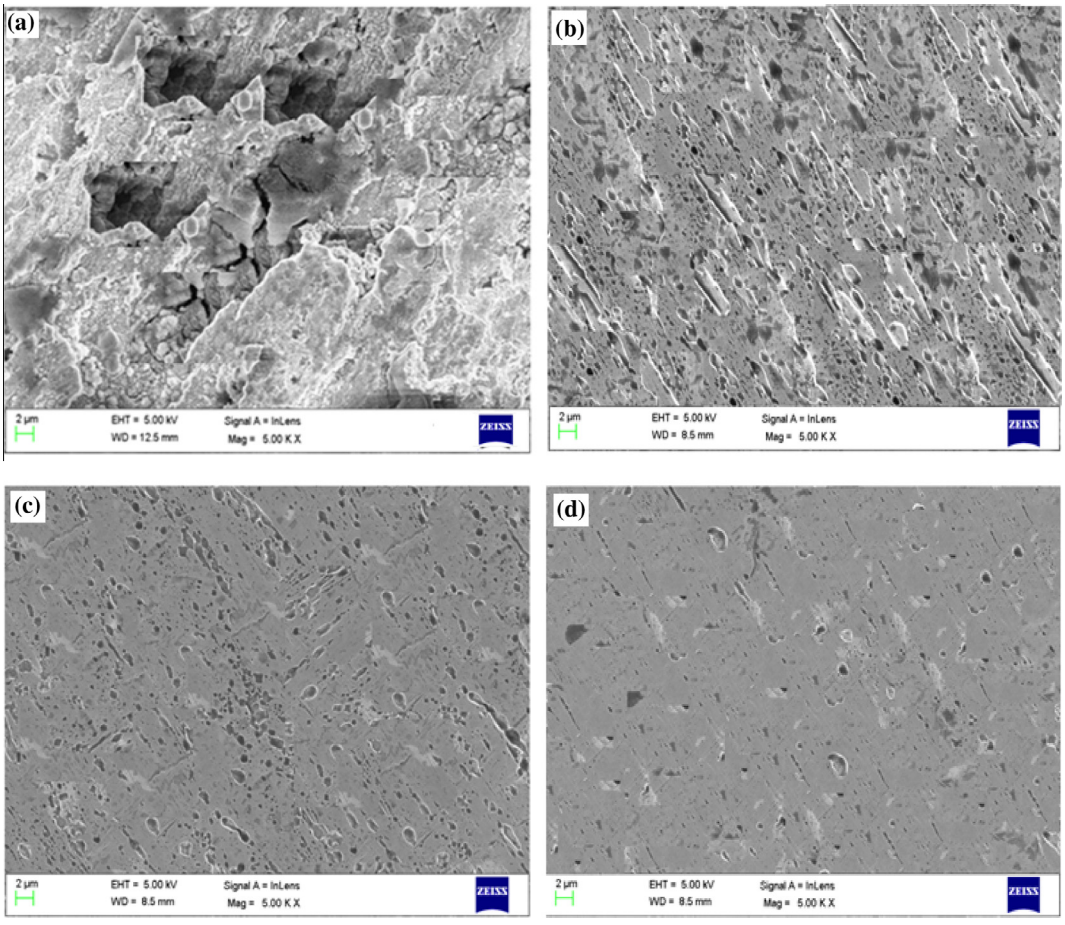

Figure 6 SEM micrographs of mild steel surfaces in the absence (a) and presence of optimum concentration of BIM-1 (b), BIM-2 (c) and BIM-3 (d).

investigation values of ΔG°_{ads} vary from −33.38 to −36.42 kJ mol^{-1} (Table 3) that signifying the both physical and chemical i.e. physiochemisorption of BIMs (Daoud et al., 2015). The negative sign of ΔG°_{ads} ensures the spontaneity of the adsorption process (Daoud et al., 2015).

3.2. Electrochemical measurements

3.2.1. Polarization study

Fig. 4 represents the Tafel polarization curves for mild steel corrosion in 1 M HCl in the absence and the presence of optimum concentration of BIMs at 308 K. The polarization parameters namely corrosion potential (E_{corr}), the corrosion current density (i_{corr}), anodic Tafel slope (β_a), cathodic Tafel slope (β_c) and corresponding η% were calculated from Tafel extrapolation method and given in Table 4. The η% was calculated using following equation:

$$\eta\% = \frac{i^{0}_{corr} - i^{i}_{corr}}{i^{0}_{corr}} \times 100 \quad (8)$$

where, i^{0}_{corr} and i^{i}_{corr} are the corrosion current densities in the absence and the presence of the BIMs, respectively. It can be observed that addition of the BIMs significantly decreases the values of i_{corr} suggesting that BIMs strongly adsorb on the mild steel surface in 1 M HCl and retard the electrochemical reaction occurring on metal surface due to the presence of protective film (Ansari and Quraishi, 2015). From Fig. 4 it can also be observed that both cathodic and anodic reactions were affected in the presence of BIMs. However, cathodic reactions are comparatively more affected than anodic reactions without causing any significant change in E_{corr} values (< 85 mV) suggesting that BIMs are mixed type but predominantly cathodic inhibitors (Anejjar et al., 2014).

3.2.2. EIS measurements

Fig. 5a represents the typical Nyquist and Bode plots in the absence and the presence of optimum concentration of the BIMs. The EIS parameters namely solution resistance (R_s), charge transfer resistance (R_{ct}), double layer capacitance (C_{dl}), and corresponding η% were calculated from EIS measurements using equivalent circuit (Fig. 5b) and given in Table 5. The increased values of R_{ct} suggest that presence of BIMs creates a barrier for mass and charge transfer process (Eddy et al., 2014). The double layer capacitance (C_{dl}) in the present study was calculated using the following relation:

$$C_{dl} = \frac{Y\omega^{n-1}}{\sin(n(\pi/2))} \quad (9)$$

where Y is the amplitude comparable to a capacitance (with a μF cm^{-2}), ω is the angular frequency, n is the phase shift, which is a measure of surface roughness. Generally, the high value of n is associated with high surface coverage. From Table 5, it is observed that values of C_{dl} decrease in the presence of BIMs which can be attributed due to decrease in the local dielectric constant and/or an increase in the thickness of electric double layer (Bammou et al., 2014).

Fig. 5c represents the Bode impedance magnitude and phase angle plot for mild steel in the absence and the presence of 200 gm L^{-1} concentration of BIMs. As seen, the Bode plot gives one time constant and shows a single maximum which is a characteristic response of mild steel corrosion in acid solution. It can be observed from the Bode plot that phase angle significantly increased in the presence of BIMs due to the formation of the protecting film by them on the mild steel surface (Verma et al., 2014). This finding suggests that adsorption of the BIMs on mild steel surface decreases the surface roughness and therefore, increases the phase angle values.

3.3. Surface investigation

3.3.1. SEM analysis

The SEM micrographs of mild steel surface after 3 h immersion are shown in Fig. 6. The surface morphology in the absence of BIMs (Fig. 6a) is damaged surface. However, in the presence of BIMs (Fig. 6b–d) the surface of mild steely significantly improved. This finding further supports that BIMs inhibit the mild steel corrosion by adsorption mechanism.

3.3.2. EDX analysis

The EDX spectra in the absence and the presence of the optimum concentration of the BIMs after 3 h immersion are shown in Fig. 7. The EDX spectrum without BIMs gives signals only for carbon (C) and Fe as shown in Fig. 7a. However, the EDX spectra of mild steel in the presence of BIMs (Fig. 7b–d) showed characteristics signal for N and O along with C and Fe. The presence of N and O in the EDX spectra suggests that BIMs inhibit mild steel corrosion by adsorbing on the mild steel surface. Moreover, intensity of N and O increases in the order: BIM-3 > BIM-2 > BIM-1

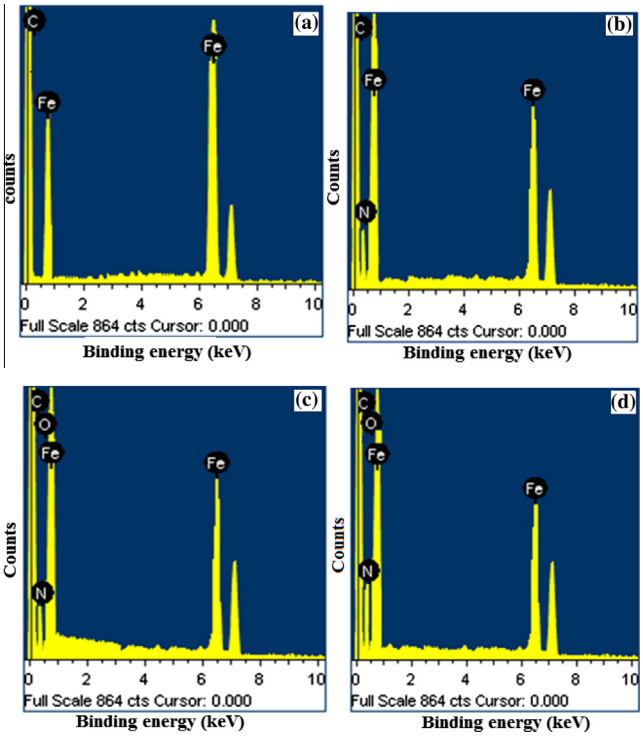

Figure 7 EDX spectra of mild steel surfaces in the absence (a) and presence of optimum concentration of BIM-1 (b), BIM-2 (c) and BIM-3 (d).

suggesting that BIM-3 has the strongest tendency to adsorb on the mild steel surface among the studied BIMs.

4. Conclusion

Results show that BIMs act as good corrosion inhibitors for mild steel in 1 M HCl and their inhibition efficiency increases with increasing concentration. The negative value of $\Delta G°_{ads}$ suggests that BIMs adsorb spontaneously and their adsorption obeys the Langmuir adsorption isotherm. The polarization study revealed that the BIMs act as mixed type inhibitors. The presence of the BIMs increases the charge transfer values and therefore inhibits mild steel corrosion. The SEM and EDX measurements well support the weight loss and electrochemical finding.

Acknowledgement

Chandra Bhan Verma gratefully acknowledges Ministry of Human Resource Development (MHRD), New Delhi (India) for providing financial assistance and facilitation for present study.

References

Anejjar, A., Salghi, R., Zarrouk, A., Benali, O., Zarrok, H., Hammouti, B., Ebenso, E.E., 2014. Inhibition of carbon steel corrosion in 1 M HCl medium by potassium thiocyanate. J. Assoc. Arab Univ. Basic Appl. Sci. 15, 21–27.

Ansari, K.R., Quraishi, M.A., 2015. Effect of three component (aniline–formaldehyde and piperazine) polymer on mild steel corrosion in hydrochloric acid medium. J. Assoc. Arab Univ. Basic Appl. Sci. 18, 12–18.

Bahrami, M.J., Hosseini, S.M.A., Pilvar, P., 2010. Experimental and theoretical investigation of organic compounds as inhibitors for mild steel corrosion in sulfuric acid medium. Corros. Sci. 52, 2793–2803.

Bammou, L., Belkhaouda, M., Salghi, R., Benali, O., Zarrouk, A., Zarrok, H., Hammouti, B., 2014. Corrosion inhibition of steel in sulfuric acidic solution by the *Chenopodium Ambrosioides* Extracts. J. Assoc. Arab Univ. Basic Appl. Sci. 16, 83–90.

Barmatov, E., Hughes, T., Nagl, M., 2015. Efficiency of film-forming corrosion inhibitors in strong hydrochloric acid under laminar and turbulent flow conditions. Corros. Sci. 92, 85–94.

Daoud, D., Douadi, T., Hamani, H., Chafaa, S., Al-Noaimi, M., 2015. Corrosion inhibition of mild steel by two new S-heterocyclic compounds in 1 M HCl: experimental and computational study. doi: http://dx.doi.org/10.1016/j.corsci.2015.01.025.

Deng, S., Li, X., Fu, H., 2011. Acid violet 6B as a novel corrosion inhibitor for cold rolled steel in hydrochloric acid solution. Corros. Sci. 53, 760–778.

Eddy, NO., Momoh-Yahaya, H., Oguzie, EE., 2014. Theoretical and experimental studies on the corrosion inhibition potentials of some purines for aluminum in 0.1 M HCl. J. Adv. Res. doi: http://dx.doi.org/10.1016/j.jare.2014.01.004.

Faustin, M., Maciuk, A., Salvin, P., Roos, C., Lebrini, M., 2015. Corrosion inhibition of C38 steel by alkaloids extract of *Geissospermum* leave in 1 M hydrochloric acid: electrochemical and phytochemical studies. Corros. Sci. 92, 287–300.

Goharshad, E.K., Ding, Y., Jorabchi, M.N., Nancarrow, P., 2009. Ultrasound-assisted green synthesis of nanocrystalline ZnO in the ionic liquid [hmim][NTf2]. Ultrason. Sonochem. 16, 120–123.

Joshi, R.S., Mandhane, P.G., Diwakar, S.D., Gill, C.H., 2010. Ultrasound assisted green synthesis of bis(indol-3-yl)methanes catalyzed by 1-hexenesulphonic acid sodium salt. Ultrason. Sonochem. 17, 298–300.

Lowmunkhong, P., Ungthararak, D., Sutthivaiyakit, P., 2010. Tryptamine as a corrosion inhibitor of mild steel in hydrochloric acid solution. Corros. Sci. 52, 30–36.

Mahdavian, M., Ashhari, S., 2010. Corrosion inhibition performance of mercaptobenzimidazole and 2-mercaptobenzoxazole compounds for protection of mild steel in hydrochloric acid solution. Electrochim. Acta 55, 1720–1724.

Musa, A.Y., Jalgham, R.T.T., Mohamad, A.B., 2012. Molecular dynamic and quantum chemical calculations for phthalazine derivatives as corrosion inhibitors of mild steel in 1 M HCl. Corros. Sci. 56, 176–183.

Norr, E.A., 2008. Comparative study on the corrosion inhibition of mild steel by aqueous extract of Fenugreek seeds and leaves in acidic solutions. J. Eng. Appl. Sci. 3, 23–30.

Ozkir, D., Kayakirilmaz, K., Bayol, E., Gurten, A.A., Kandemirli, F., 2012. The inhibition effects of Azure A on mild steel in 1 M HCl. A complete study: adsorption, temperature, duration and quantum chemical aspects. Corros. Sci. 56, 143–152.

Popova, A., Christov, M., 2006. Evaluation of impedance measurements on mild steel corrosion in acid media in the presence of heterocyclic compounds. Corros. Sci. 48, 3208–3221.

Quartarone, G., Battilana, M., Bonaldo, L., Tortato, T., 2008. Investigation of the inhibition effect of indole-3-carboxylic acid on the copper corrosion in 0.5 M H2SO4. Corros. Sci. 50, 3467–3474.

Solmaz, R., 2014. Investigation of corrosion inhibition mechanism and stability of vitamin B1 on mild steel in 0.5 M HCl solution. Corros. Sci. 81, 75–84.

Sonar, S.S., Sadaphal, S.A., Kategaonkar, A.H., Pokalwar, R.U., Shingate, B.B., Shingare, M.S., 2009. Alum catalyzed simple and efficient synthesis of bis(indolyl)methanes by ultrasound approach. Bull. Korean Chem. Soc. 30, 825–828.

Surasani, R., Kalita, D., Chandrasekhar, K.B., 2013. Indion Ina 225H resin as a novel, selective, recyclable, eco-benign heterogeneous catalyst for the synthesis of bis(indolyl) methanes. Green Chem. Lett. Rev. 6, 113–122.

Verma, C.B., Quraishi, M.A., Singh, A., 2014a. 2-Aminobenzene-1,3-dicarbonitriles as green corrosion inhibitor for mild steel in 1 M HCl: electrochemical, thermodynamic, surface and quantum chemical investigation. J. Taiwan Inst. Chem. Eng. 2014, 1–11. http://dx.doi.org/10.1016/j.jtice.2014.11.029.

Verma, C.B., Reddy, M.J., Quraishi, M.A., 2014b. Microwave assisted eco-friendly synthesis of chalcones using 2,4-dihydroxyacetophenone and aldehydes as corrosion inhibitors for mild steel in 1 M HCl. Anal. Bioanal. Electrochem. 6, 321–340.

Yadav, M., Behera, D., Kumar, S., Sinha, R.R., 2013. Experimental and quantum chemical studies on the corrosion inhibition performance of benzimidazole derivatives for mild steel in HCl. Ind. Eng. Chem. Res. 52, 6318–6328.